

SANDIA REPORT

SAND2010-4671
Unlimited Release
Printed July 2010

Expected Result of Firing an ICE Load on Z without Vacuum

Kenneth W. Struve, Raymond W. Lemke, Mark E. Savage

Prepared by
Sandia National Laboratories
Albuquerque, New Mexico 87185 and Livermore, California 94550

Sandia National Laboratories is a multi-program laboratory managed and operated by Sandia Corporation, a wholly owned subsidiary of Lockheed Martin Corporation, for the U.S. Department of Energy's National Nuclear Security Administration under contract DE-AC04-94AL85000.

Approved for public release; further dissemination unlimited.

Issued by Sandia National Laboratories, operated for the United States Department of Energy by Sandia Corporation.

NOTICE: This report was prepared as an account of work sponsored by an agency of the United States Government. Neither the United States Government, nor any agency thereof, nor any of their employees, nor any of their contractors, subcontractors, or their employees, make any warranty, express or implied, or assume any legal liability or responsibility for the accuracy, completeness, or usefulness of any information, apparatus, product, or process disclosed, or represent that its use would not infringe privately owned rights. Reference herein to any specific commercial product, process, or service by trade name, trademark, manufacturer, or otherwise, does not necessarily constitute or imply its endorsement, recommendation, or favoring by the United States Government, any agency thereof, or any of their contractors or subcontractors. The views and opinions expressed herein do not necessarily state or reflect those of the United States Government, any agency thereof, or any of their contractors.

Printed in the United States of America. This report has been reproduced directly from the best available copy.

Available to DOE and DOE contractors from
U.S. Department of Energy
Office of Scientific and Technical Information
P.O. Box 62
Oak Ridge, TN 37831

Telephone: (865) 576-8401
Facsimile: (865) 576-5728
E-Mail: reports@adonis.osti.gov
Online ordering: <http://www.osti.gov/bridge>

Available to the public from
U.S. Department of Commerce
National Technical Information Service
5285 Port Royal Rd.
Springfield, VA 22161

Telephone: (800) 553-6847
Facsimile: (703) 605-6900
E-Mail: orders@ntis.fedworld.gov
Online order: <http://www.ntis.gov/help/ordermethods.asp?loc=7-4-0#online>



SANDIA REPORT

SAND2010-4671
Unlimited Release
Printed July 2010

Expected Result of Firing an ICE Load on Z without Vacuum

Kenneth W. Struve, Raymond W. Lemke, Mark E. Savage

Center 1600
Sandia National Laboratories
PO Box 5800
Albuquerque, NM 87185-1194

Abstract

In addressing the issue of the determining the hazard categorization of the Z Accelerator of doing SNM experiments the question arose as to whether the machine could be fired with its central vacuum chamber open, thus providing a path for airborne release of SNM materials. In this report we summarize calculations that show that we could only expect a maximum current of 460 kA into such a load in a long-pulse mode, which will be used for the SNM experiments, and 750 kA in a short-pulse mode, which is not useful for these experiments. We also investigated the effect of the current for both cases and found that for neither case is the current high enough to either melt or vaporize these loads, with a melt threshold of 1.6 MA. Therefore, a necessary condition to melt, vaporize, or otherwise disperse SNM material is that a vacuum must exist in the Z vacuum chamber. Thus the vacuum chamber serves as a passive feature that prevents any airborne release during the shot, regardless of whatever containment may be in place.

Contents

1. Introduction	7
2. Expected Current to a short-circuit load on Z	7
2.1. Likely breakdown locations	8
2.2. Number of arcs expected	10
2.3. Circuit-Code Simulations	11
2.4. Inferred Peak Current	12
3. Effect of low currents on an ICE-type load on Z	12
3.1. Result of a failed Z shot with only 450 kA through the load	14
3.2. Estimates of Surface Heating and Melting	15
3.3. Peak Pressure vs. Peak Current	17
3.4. MHD Simulation of the Pu ICE Load with a 500 kA Current	18
4. Conclusions	21
5. References	22
Appendix A. Review of the Peak Current Prediction	23

Terms

Z – Refers to the Z Accelerator in building 983, Sandia National Laboratories

ICE – Isentropic Compression Experiment, i. e., a process in which there are no irreversible dissipative processes, such as shock wave propagation.

MITL – Magnetically Insulated Transmission Line. A vacuum transmission line where the self-current driven magnetic field is sufficient to prevent electron emission from crossing the transmission line gap and shorting the line.

SNM -- Special Nuclear Material. Special nuclear material" (SNM) is defined by Title I of the Atomic Energy Act of 1954 as plutonium, uranium-233, or uranium enriched in the isotopes uranium-233 or uranium-235.

PHC – Post-Hole Convolute. The parallel connection of the four MITLs of the Z vacuum section that add currents from each of the lines. Anode posts pass through holes in the cathodes to connect the parallel anodes. Hence the name.

MHD – Magneto Hydro Dynamic. Refers to a fluid-equation description of a plasma that also includes electric and magnetic fields.

1. Introduction

With the possibility of doing Special Nuclear Materials experiments on Z, where the vacuum chamber provides passive protection against accidental release of vaporized materials, it is prudent to verify that the Z accelerator cannot deliver sufficient current and energy to an ICE-type load to vaporize and cause an accidental release if the vacuum were open or a vacuum condition not established. Therefore, the following examines what current could be expected through a short-circuit load if the vacuum chamber were not evacuated but left at atmospheric air pressure. The Z MITLs rely on magnetic insulation in vacuum to transmit current to a load, and can support fields exceeding many megavolts per centimeter. Without a vacuum, electrons emitted from a cathode surface cannot be bent back to the electrode by the magnetic field before colliding with air molecules, knocking off more electrons, and initiating an avalanche process leading to a vacuum arc. That is, magnetic insulation cannot exist if the mean-free-path for electron-neutral collisions is much less than the electron gyroradius. Therefore, we expect that little if any current could reach a load containing special nuclear materials, and could not cause loss of confinement if the primary containment system were to fail. Thus a necessary requirement to deliver sufficient energy to the load to vaporize and disperse materials is that a vacuum must exist in the Z vacuum chamber. Thereby the Z vacuum chamber becomes a passive design feature that must exist before load material can be vaporized.

2. Expected Current to a short-circuit load on Z

If the Z vacuum chamber were breeched and Z fired at full atmospheric air pressure, it is only possible to get a small current to a load. The analysis involves determining where and when the electrodes are shorted by arcing, how many parallel arcs can be initiated, their resistance and inductance, and determining how these parallel current paths affect the current delivered to the load, which is also a short circuit. These parameters are then used in the validated circuit model of Z to predict what current might reach the load.

2.1. Likely breakdown locations

Pulsed breakdown in air can be expected at about 30 kV/cm for the short pulse ($\tau_r \approx 100$ ns) operation of Z, and 22 kV/cm for long-pulse ($\tau_r \approx 600$ ns) [1]. Potential sites for breakdown are thus at (1) the air side of the vacuum insulator stack, (2) the end of the vacuum flare where the MITL narrows to a small gap, (3) throughout the constant impedance section of the MITL, (4) the constant-gap portion of the MITL near the post-hole convolute, and (5) the post-hole convolute (PHC). See figs. 1 and 2 for these locations. Mean electric field expected at each of these locations is shown in fig. 3, which consists of voltages extracted from a Bertha simulation of Z shot 1780 [2], divided by the gap at that location. At the PHC the field shown is twice the average field because of the enhancement caused by the diameter of the posts and the relatively sharp edge of the cathode hole through which the post passes. The simulation for this shot, which was a short-pulse, short-circuit shot with a peak current of 26 MA, matches the measured load waveform and current to within one per cent through peak current. As can be seen, the highest fields occur at the PHC, but breakdown can be expected at any of the other locations since all exceed the breakdown limits in air. But, as an estimate, we only consider arcing at the

end of the vacuum flare and at the PHC, realizing that an arc at those locations will reduce voltage throughout the MITLs and at the stack, thus limiting the number of arc locations.

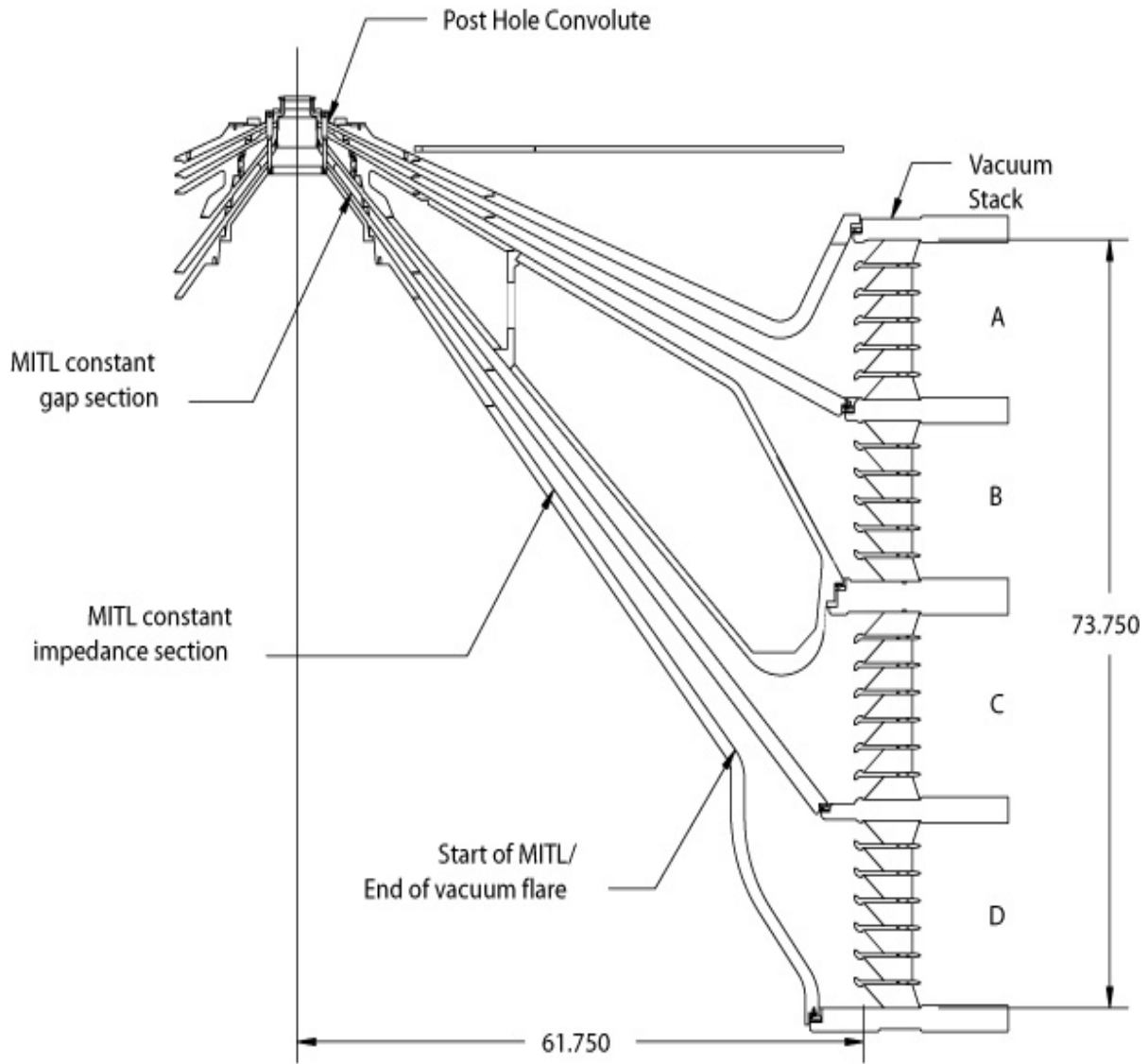


Figure 1. Geometry of the Z vacuum stack and MITLs. Dimensions in inches.

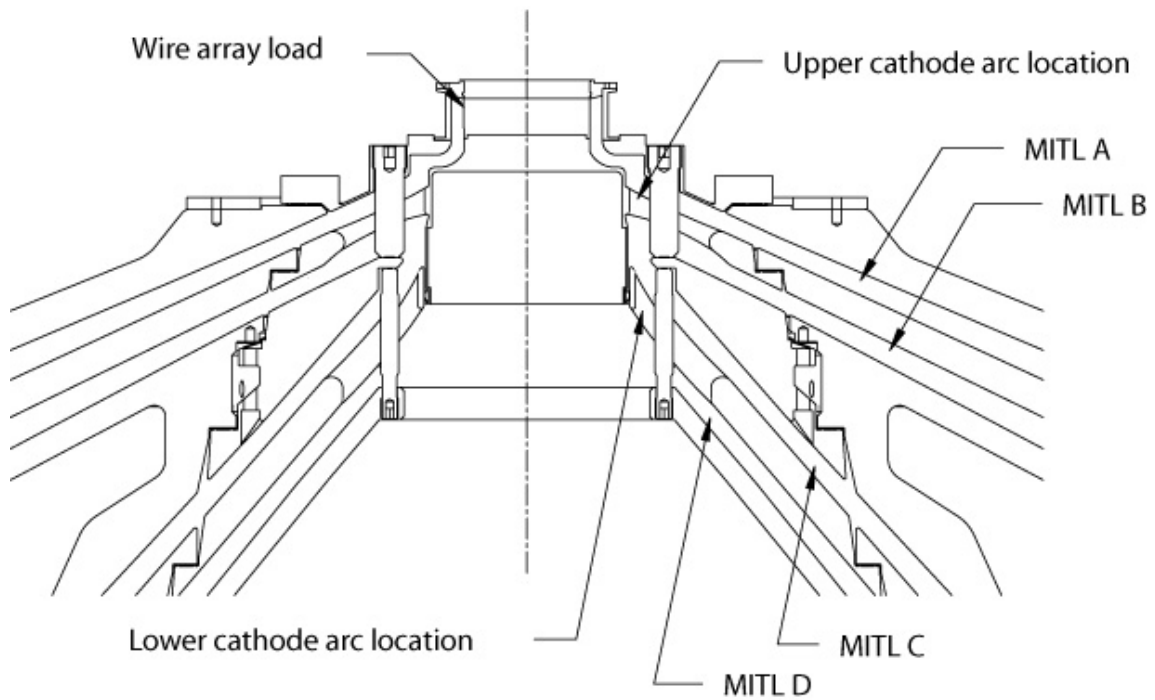
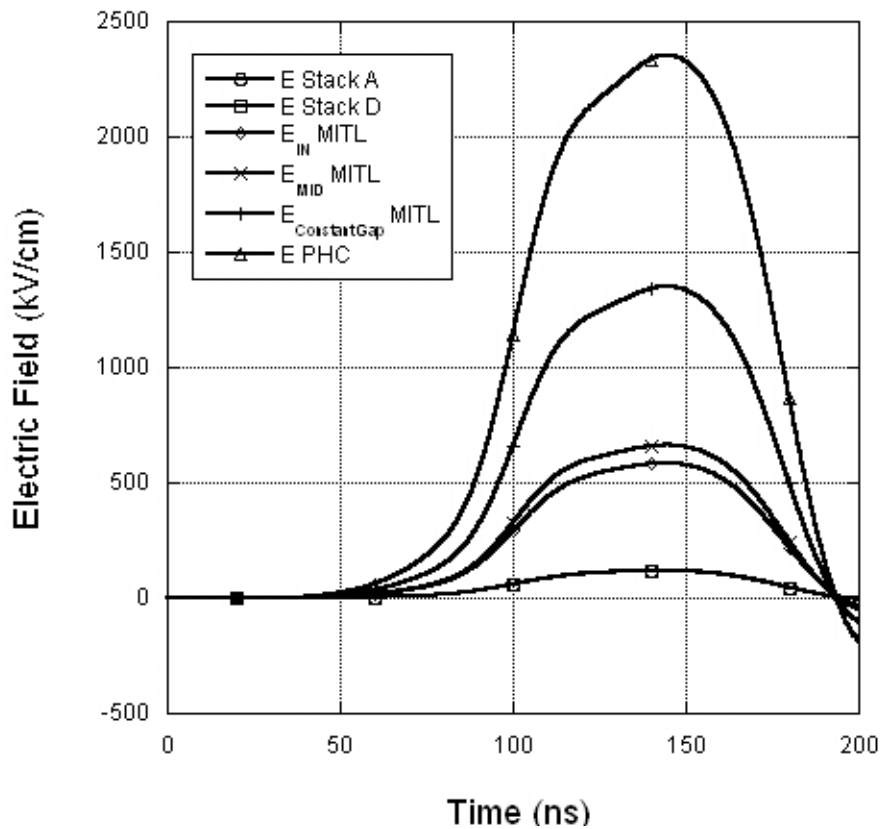


Figure 2. Post-hole convolute. Highest fields in the cathode/anode-post gap locations.



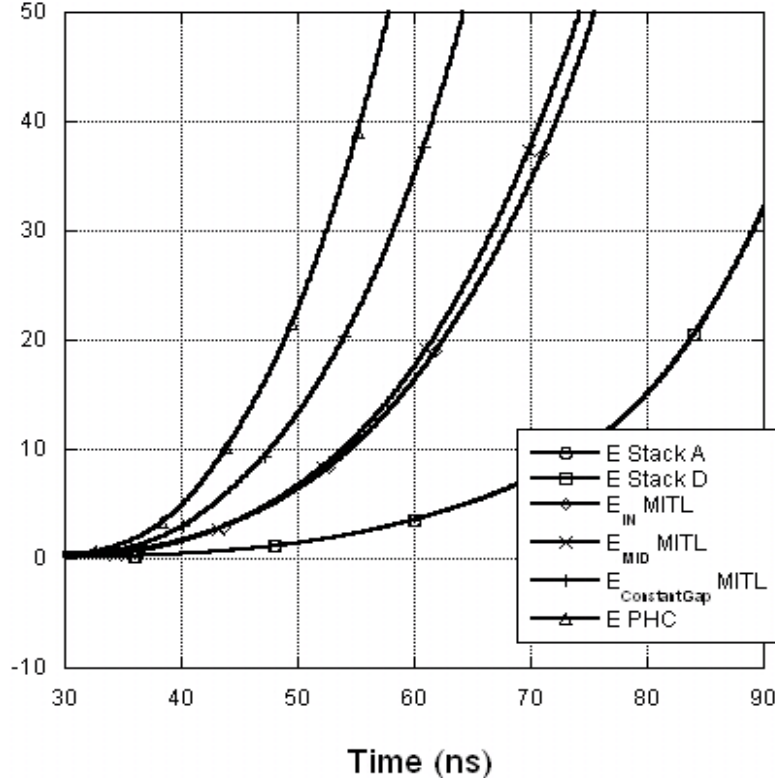


Figure 3. Electric field at several locations in the vacuum section, from Bertha simulation of Z shot 1780.

2.2. Number of arcs expected

After-shot inspection of the Z PHC hardware shows that for every shot there is arcing from the anode posts to the cathode holes through which they pass. For the 12-post design, there are 24 arc locations, which is the number of arcs that can also be expected if there is air in the chamber. The inductance of the arcs can be estimated using an expression for the inductance of a finite-length straight wire given by Grover [3]. This expression gives the inductance of a 10 mm long, 1 mm diameter arc as 5.9 nH, or an equivalent inductance of 0.25 nH for 24 arcs. The arc resistance is calculated in Bertha using the Tom Martin switch model [4], which is based on the expansion of an arc channel using the Braginskii formulation [5]. Bertha simulations show that even with 24 parallel arcs inductance and resistance is sufficient that the electric field in the PHC still exceeds the breakdown field.

Simulations also show that even with breakdown at the PHC there can still be sufficient voltage developed to cause breakdown at the start of the narrow-gap section of the MITLs. This is a result of the inductance between the PHC and that location. The number of independent arcs can be estimated using an expression developed by JC Martin that expresses how long it can take for an arc at one location to prevent arcing at another [6]. The number n of independent channels can be expressed as

$$2\sigma T = 0.1\tau_{tot} + 0.8\tau_{trans} , \quad (1)$$

where $2\sigma T$ is the uncertainty in the time of breakdown, which is approximately 2 ns for a 100 ns rise-time pulse, τ_{tot} is time that voltage can be reduced by inductance and resistive of the arc, and τ_{trans} is the delay time between arc locations. Both τ_{tot} and τ_{trans} are functions of n . Ignoring τ_{tot} , which only increases the number of channels, I estimate the minimum number of channels using the second term on the RHS of eq. (1). The time τ_{trans} is $2\pi r/(nc)$, the circumference of the MITL divided by n times the azimuthal velocity. For $2\sigma T = 2$ ns I find that the minimum number of channels than can be expected is 10. The inductance of each channel is estimated with the same formula from Grover, and is 43 nH each for A and B levels, and 66 nH for C and D. For the resistance I use the same model in Bertha. The time of arc initiation at the entrance to the MITLs is 15 ns later than that of the PHC.

2.3. Circuit-Code Simulations

All full-circuit model of Z was done using the short-circuit load configuration and machine setup of Z shot 1780, but with arc channels inserted at the PHC and the input to the MITLs, as described above. A comparison of the currents both with and without arcs is shown in fig. 4. Note that the peak current at the load with arcing is about 750 kA. The electric field at the MITL and PHC arc locations is shown in fig. 5. Note, that even with the voltage reduced at these locations, arcing is still likely at later times. Also note, that the timing of the arcs is somewhat artificial in the simulation since the arcs are inserted as equivalent arcs on each MITL, and one equivalent arc at the PHC. More likely, the start time of each individual arc would be different as the voltage drive pulse rises. Thus, the sharp drop in field noted at the time of breakdown, as seen in fig. 5, would probably not be seen in an actual experiment.

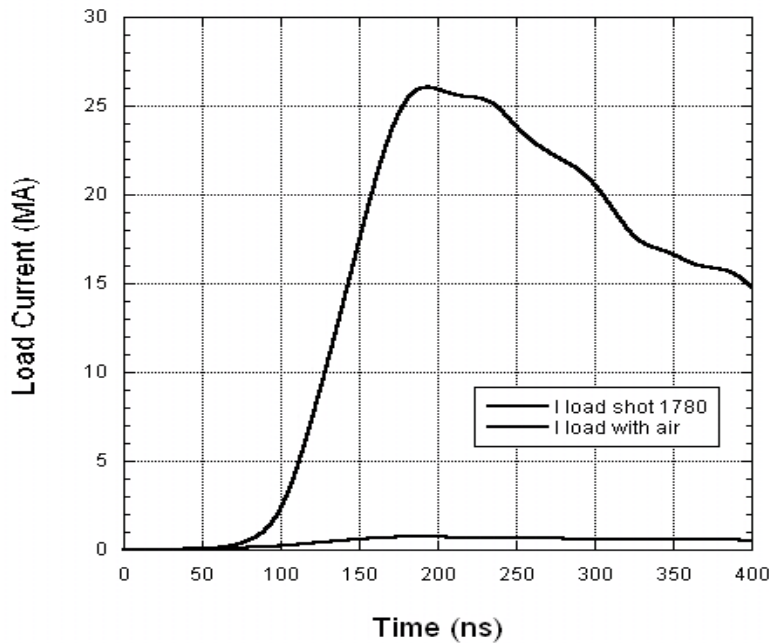


Figure 4. Circuit-code prediction of load current with and without arcing at the PHC and the input to the MITLs.

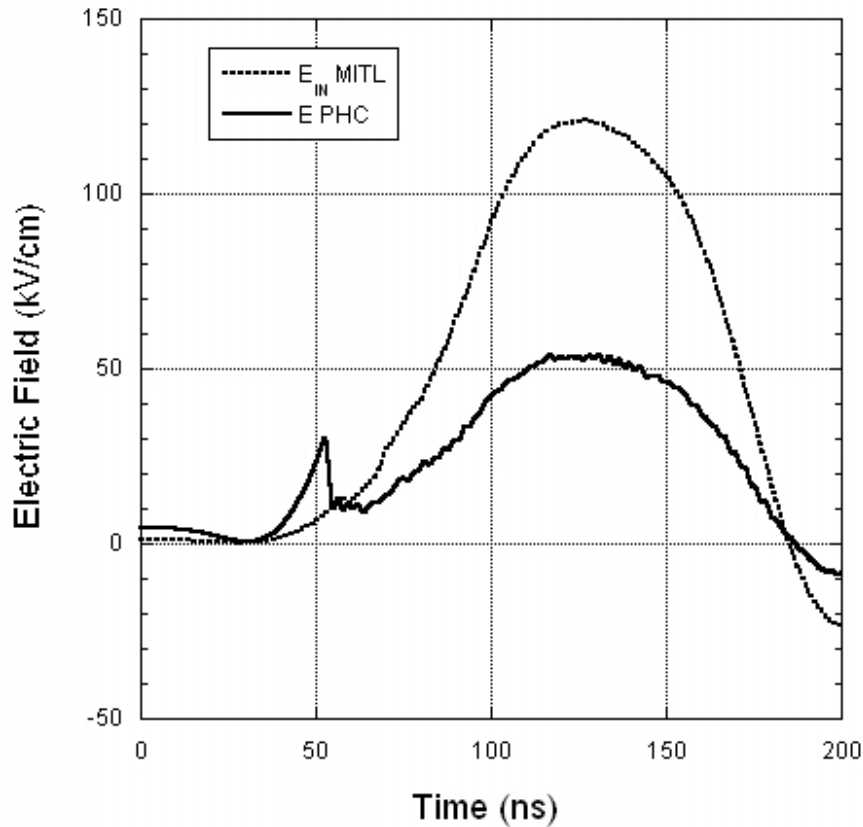


Figure 5. Electric field at the PHC and the input to the MITLs with arcing at those locations.

2.4. Inferred Peak Current

In the worst case, we expect that the Z accelerator can deliver at most a maximum of 750 kA into a load if the vacuum chamber were filled with air at atmospheric or partial pressure. More than likely, more arcs will be initiated than here simulated, and current would be even less. These simulations were done for Z in the short pulse mode. For ICE shots the accelerator is operated in a long pulse mode with a peak current of 16 MA. With scaling by the ratio of the peak currents of the two modes we expect a peak current of no greater than 460 kA for the plutonium ICE shots. An independent evaluation of this result is given by Mark Savage in Appendix A.

3. Effect of a low current on an ICE load on Z

Questions remain concerning how much damage could still be done by this current. Could the load hardware be vaporized and spread material throughout the chamber? How does this damage scale with peak current?

In answering these questions we consider the ICE load configuration planned for the plutonium shots, where the current through aluminum electrodes generates a magnetic field pressure that presses on a plutonium sample located behind the current-carrying surface. Fig. 6 shows a 3D

rendering of the load, with side electrodes and cathode removed, and fig. 7 shows a 2D cross section through the plutonium sample.

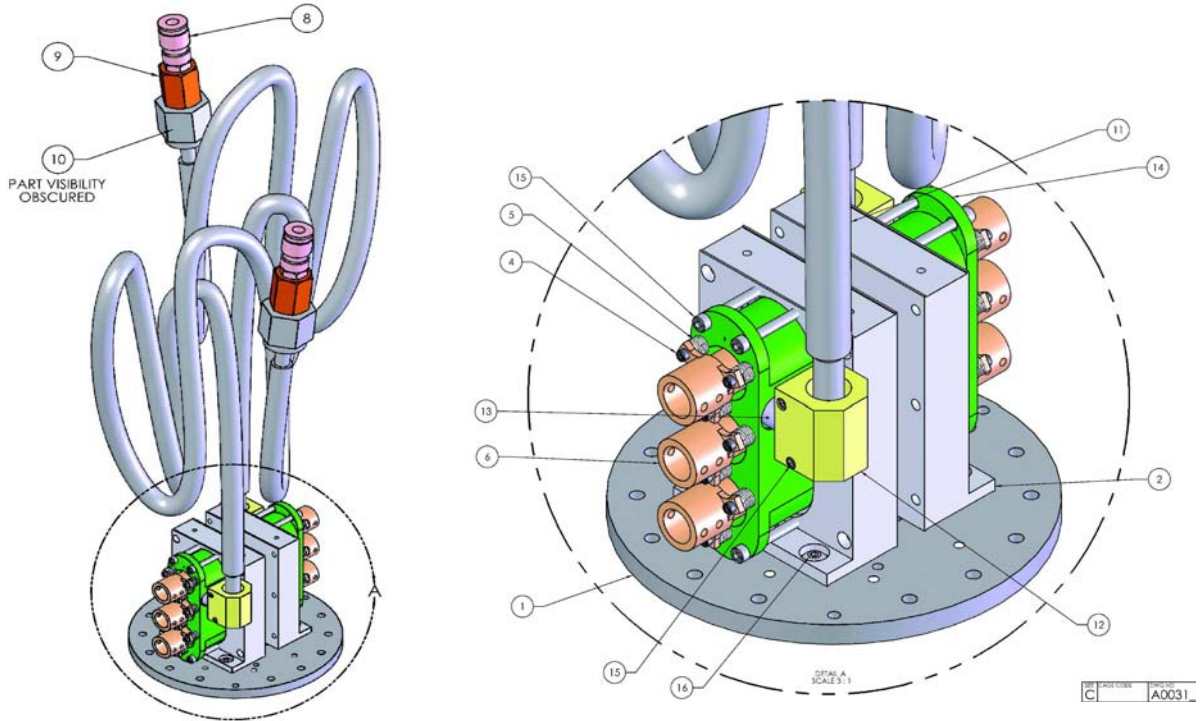


Figure 6. ICE load configuration planned for plutonium shots on Z. Shown are the two aluminum anode conductors (45 x 60 mm) that contain the Pu samples. Not shown are the cathode, two anode side conductors, and a shorting block on the top.

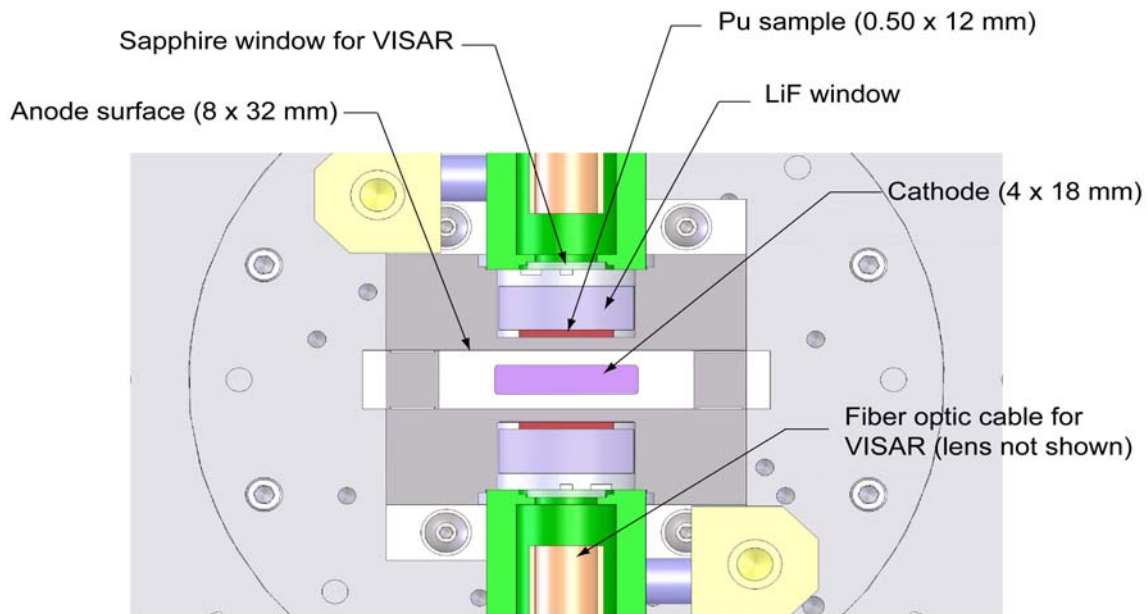


Figure 7. Cross-section of the Pu ICE load planned for shots on Z.

Several approaches are used to address these issues. The first is to compare to a failed ICE shot, Z shot 1931, where only one out of thirty-six lines was triggered, resulting in only 450 kA getting to the load. This shot showed only minor melting and no loss of material from the current-carrying surfaces, which were aluminum. The second is to estimate the energy loss into the conductors of an ICE load as a function of peak current, and use these estimates to predict surface melting or vaporization of the current-carrying conductors. The third is to estimate peak magnetic field energy and to determine if pressures exceed the yield strength of the materials. A fourth approach is to use a 2D MHD code to simulate current flow, resistive heating, and material deformation for these low currents.

3.1. Result of a failed Z shot with only 450 kA through the load

The configuration for Z shot was a single strip-line ICE load as shown in fig. 8. For this configuration the current density was four-times higher than would be in a Pu ICE load at the same current. The conductors were 11-mm wide, rectangular aluminum strip-line conductors shorted at one end and separated by 1 mm. Current flowing in the lines generated a magnetic field that broke away the 0.9 mm thick panels and accelerated them toward the quartz and sapphire plates, located 6.1 mm behind the panels. With this shot only one line of Z triggered, resulting in only 450 kA peak current getting to this load. A picture of the load after the shot is shown in fig. 9. The panels broke away from the electrodes, and impacted the brittle quartz and sapphire disks, pulverizing them. The white material seen in the photograph is the pulverized quartz and sapphire. Inspection of the electrodes after the shot showed only minor melting of the aluminum surfaces and no material loss. There was however mechanical deformation of the aluminum electrodes from the magnetic pressure. Thus, at four times the current density of a Pu ICE shot in air at 450 kA, only minor electrode damage and some melting is seen. But with the Pu ICE configuration even such minor damage is not be expected.

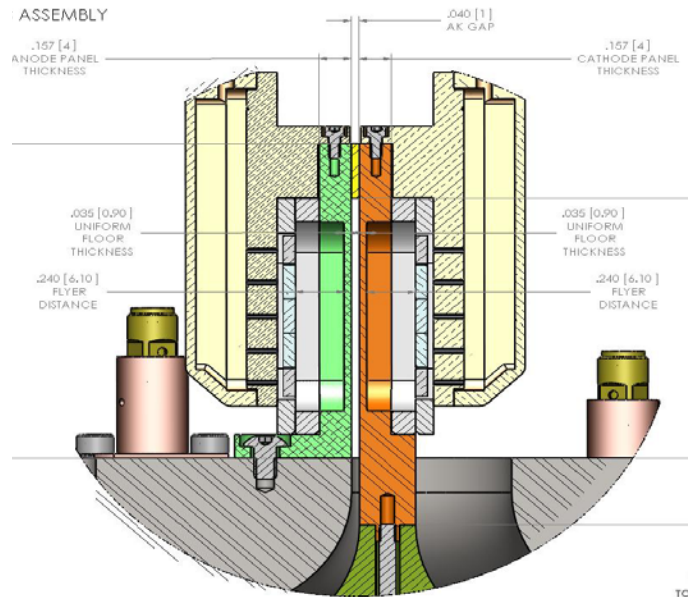


Figure 8. Cross-section of the ICE load for Z shot 1931.



Figure 9. Z shot 1931 hardware after a shot with a peak current of 450 kA. The white material seen in the photograph is pulverized quartz and sapphire. Current density for this configuration was four-times greater than would be seen with a similar current with a Pu ICE load.

3.2. Estimates of Surface Heating and Melting

In addition to comparing with experiments on Z, we can also estimate scaling of melting and potential vaporization of the electrodes as a function of current. The calculation is conservative since it assumes constant heat capacity with temperature, no thermal transport, and that the current density falls as $e^{-y/\delta}$ in the conductor where y is depth and δ is the skin depth. Using the same geometry shown in fig. 7, which is the rectangular coaxial configuration, we can calculate the energy per mass deposited into the conductors with a skin depth δ ,

$$\delta = \sqrt{\frac{\rho}{\pi\mu_0 f}} \quad , \quad (2)$$

where ρ is the electrical resistivity, f the frequency ($f = 1/(4t_{peak})$), and $\mu_0 = 4\pi \times 10^{-7}$ H/m. In a volume of the conductor with width w and length x with thickness Δy at a depth y , with current flowing in the x direction, the power P dissipated per mass m is

$$\frac{P(y,t)}{m} = \frac{(i(t))^2 R}{m} = \frac{\left(\frac{I(t)}{\delta} e^{-y/\delta} \Delta y\right)^2 \left(\frac{\rho x}{w \Delta y}\right)}{\rho_m w x \Delta y} = \frac{\pi \mu_0 f}{\rho_m} \left(\frac{I(t)}{w}\right)^2 e^{-2y/\delta} \quad , \quad (3)$$

where ρ_m is the mass density and R is resistance. Averaging over a skin depth gives

$$\frac{P(t)}{m} = \frac{\pi \mu_o f}{2\rho_m} J^2, \quad (4)$$

where J is the linear current density $I(t)/w$ in the x direction. The justification for averaging over the skin depth is that we have neglected thermal diffusion in this calculation, and with the small skin depths and the relatively long pulse length we can expect some averaging of the energy deposition in depth. To find the energy E dissipated per mass we integrate over time using a current profile that rises linearly to a peak in a time t_{peak} , and falls exponentially to zero with a time constant τ .

$$\frac{E}{m} = \int_0^\infty \frac{P(t)}{m} dt = \frac{\pi \mu_o J_o^2}{2\rho_m} \left[f_{rise} \int_0^{t_{peak}} \left(\frac{t}{t_{peak}} \right)^2 dt + f_{fall} \int_{t_{peak}}^\infty e^{-\frac{2(t-t_{peak})}{\tau}} dt \right] = \frac{k J_o^2}{\rho_m} \quad (5)$$

where $k = 7\pi\mu_o/24$ and J_o is the peak linear current density. Note that because the mass in the problem is also a function of the skin depth, the energy deposited per mass is *independent of the frequency and electrical resistivity*. This of course is only valid for frequencies and conductivities where the skin depth does not exceed the thickness of the material, and for a resistivity that does not change with temperature or phase. A more accurate calculation must be done with codes where these parameters, as well as heat capacity, can vary with temperature, and where thermal diffusion can be included. But in spite of these limitations, eq. (5) provides useful estimates for situations where material melting or vaporization might be expected.

With aluminum electrodes with the configuration shown fig. 7, we use eq. (5) to estimate current to raise the temperature to melt, current needed to melt, and also to heat to vaporization. For aluminum the relevant physical parameters are given in table 1.

Table 1. Physical parameters for Aluminum

Electrical resistivity	0.0282 $\mu\Omega\text{-m}$
Melt temperature	933 $^\circ\text{K}$
Vaporization temperature	2714 $^\circ\text{K}$
Mass density	2700 kg/m^3
Heat capacity	897 $\text{J/kg-}^\circ\text{K}$
Heat of fusion (melt)	398 kJ/kg
Heat of vaporization	10.9 MJ/kg

The energy per mass needed to raise the temperature to melt is 574 kJ/kg ($= c_p\Delta T$). Melting requires an additional 398 kJ/kg , and to start vaporization requires 1600 kJ/kg .

E/m as a function of peak current for the aluminum electrodes rises as the square of the current density, as shown in fig. 10 for $w = 44$ mm. Also shown is the energy per mass required to reach the phase boundaries. Melting can begin with a peak current of 1.6 MA, and requires a peak current of 2.1 MA to completely melt. To raise the temperature of the melted aluminum to vaporization within a skin depth requires a peak current of 3.4 MA. Thus, with a peak current of only 460 kA the energy deposited into the electrodes is 46.6 kJ/kg, which equates to a temperature rise of 52 K. No melting is expected.

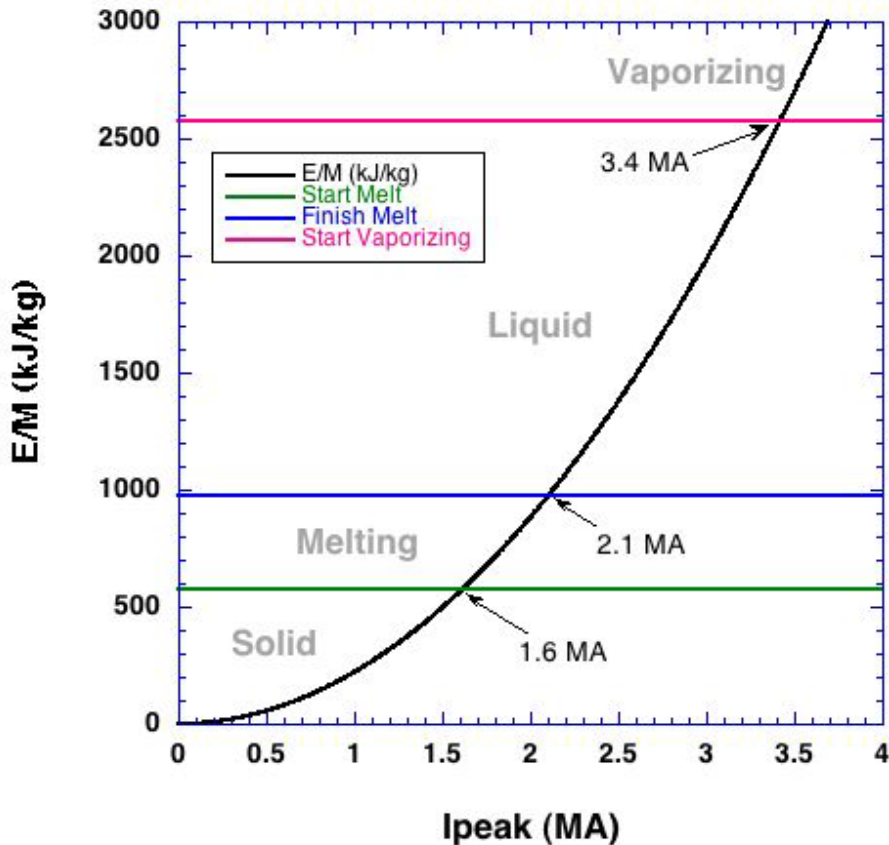


Figure 10. Energy per mass into aluminum electrodes, as estimated using eq. (5), deposited into one skin depth of 44 mm wide conductors as a function of the peak current with a profile that rises linearly to peak, and falls exponentially.

3.3. Peak Pressure vs. Peak Current

The peak pressure on the electrodes can also be expressed as a function of the current density. Using Ampere's law, and integrating along the cathode surface, which gives a conservative estimate, the peak magnetic field $B_o = \mu_o J_o$ where J_o is I_o/w , the peak current divided by the circumference of the cathode. The peak magnetic pressure $P_o = B_o^2/2\mu_o = \mu_o J_o^2/2$. The magnetic field versus current for a load with $w = 44$ mm is shown in fig. 11. Note that the yield strength of aluminum is 280 GPa, which is only exceeded for currents of 930 kA or higher. For

comparison, the yield strength of plutonium is 480 MPa at room temperature [7], and the yield strength of lithium fluoride is 11 MPa [8]. Thus, for peak current less than 930 kA we expect no deformation and only elastic motion of the aluminum electrodes, fracturing of the lithium fluoride windows, and no damage to the plutonium samples.

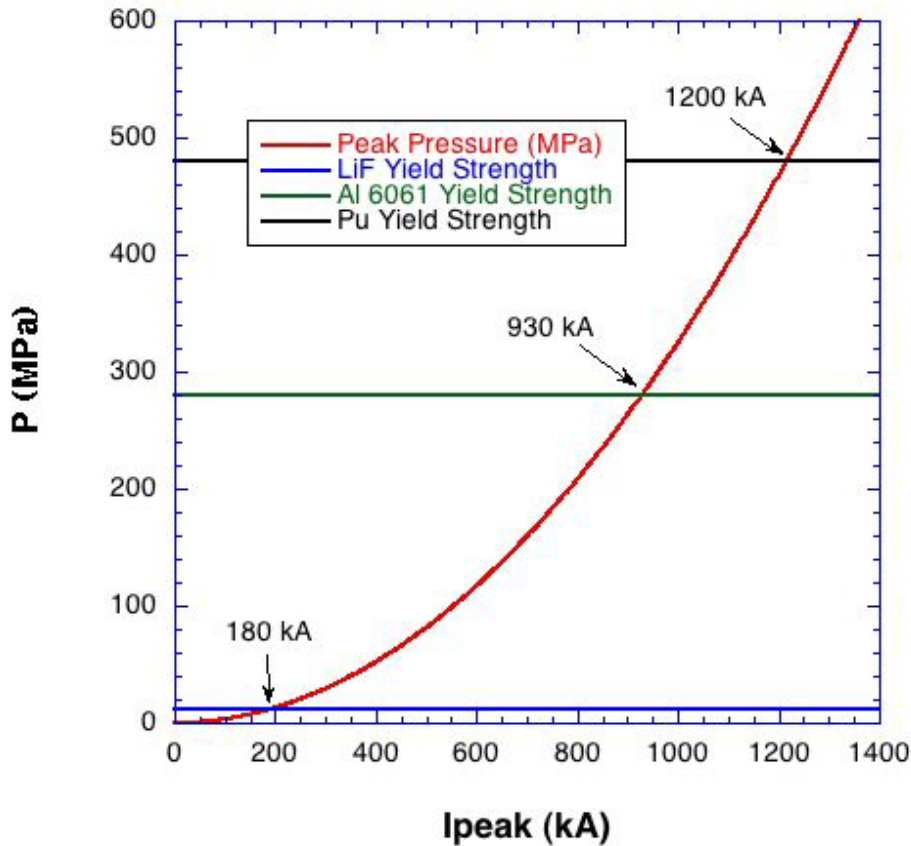


Figure 11. Peak pressure on the Pu ICE experiment vs. peak current.

3.4. MHD simulation of the Pu ICE load with a 500 kA current

To verify the estimates made with the scaling arguments of the previous sections, we have done 2D simulations of the electrode configuration shown in fig. 7 using the ALEGRA code. [9] Results of these simulations are shown in figs. 12 -14. Fig. 12 shows the electrode configuration 7 μ s after the start of current, indicating no electrode deformation. This time is well past the 500-kA peak current for the simulation. The solid colors show the density regions. The colored lines give the magnitude of the magnetic field and show field diffusion into the electrodes. The flare of the gap on the right and left sides is intentional, but does not affect results at the sample location. It helps control material jetting issues with higher-current simulations.

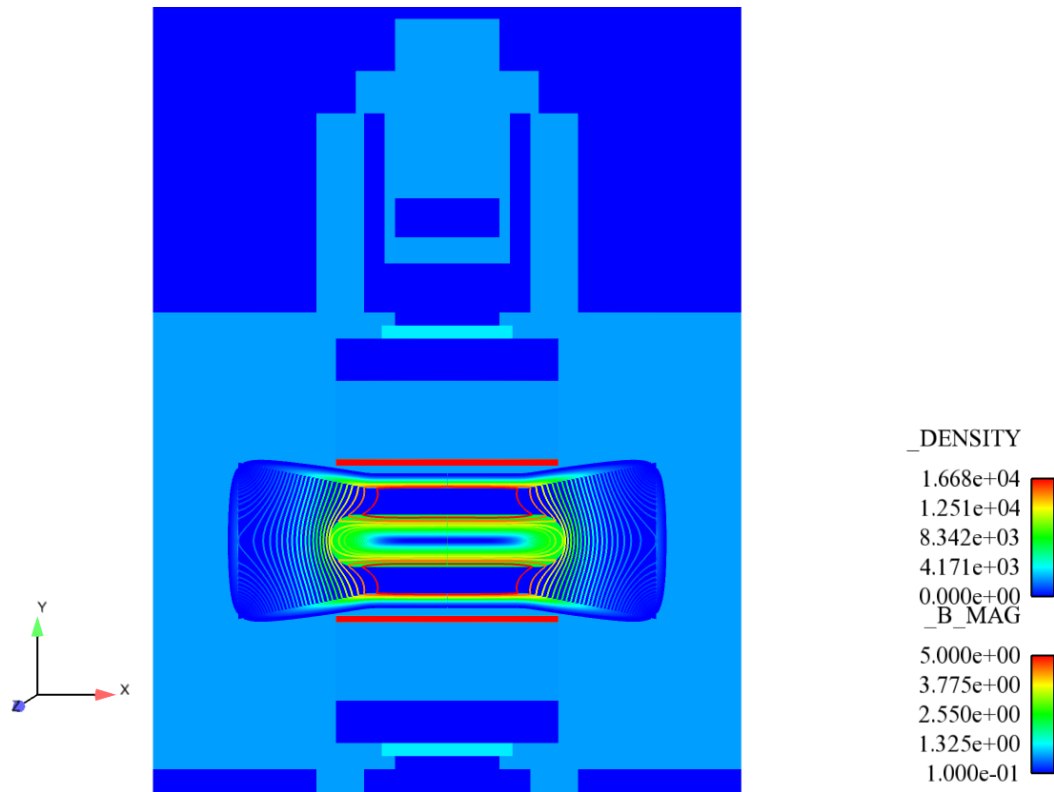


Figure 12. Plot from an ALEGRA simulation of the Pu ICE load with a peak current of 500 kA, 7 μ s after start of current, showing no mechanical deformation of the electrodes.

In fig. 13 we see the current used in the simulation to drive the load, and the calculated magnetic field pressure at the anode face. Note that the peak pressure agrees with the estimates shown in fig. 11. As noted in the previous section, the peak pressure is much less than the 280 MPa yield strength of aluminum. Fig. 14 shows the calculated mass density and temperature of the aluminum surface. The simulation shows a temperature rise of 44 K to 337 K, well below its melting temperature of 933 K. Scaling this temperature rise with the square of the current extrapolates that melt would not start until peak current exceeds 1.9 MA. This is even more conservative than the estimates of section 3.2 which predict an energy deposition into the conductors that raises the electrode temperature 61 K for a 500 kA peak current and predicts a current of 1.6 MA needed to melt. Thus, the 2D simulation shows that at 500 kA or lower we can expect no deformation of the electrode structure, pressure is well below the yield strength of aluminum, and there is no melting of the electrodes.

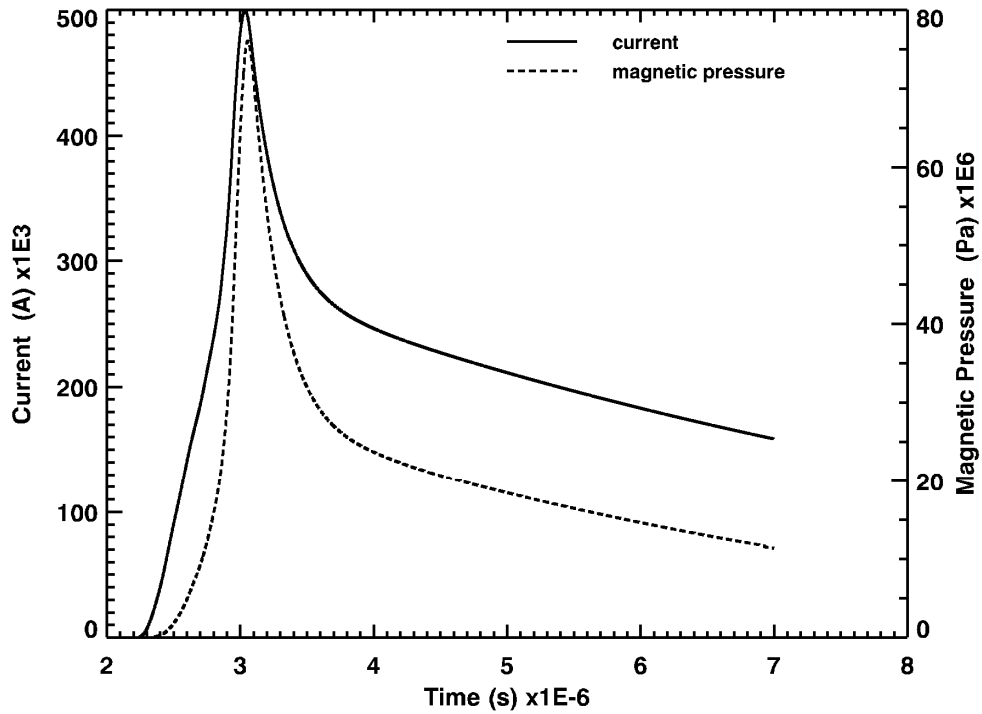


Figure 13. Applied current and calculated magnetic pressure from the ALEGRA simulation.

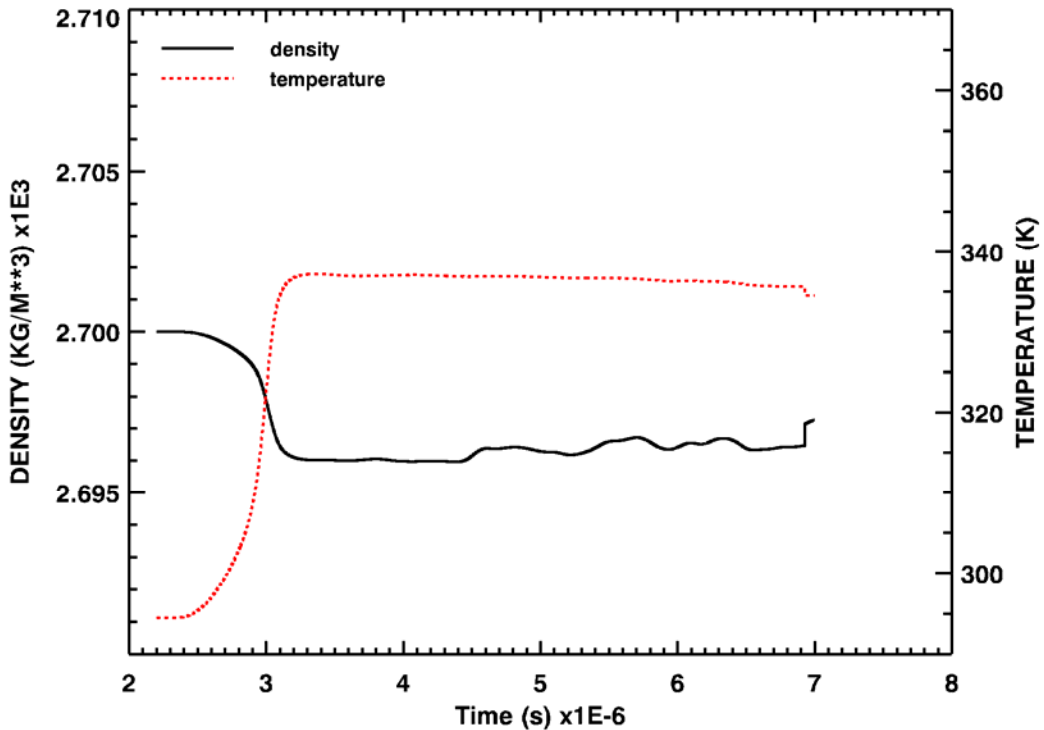


Figure 14. Calculated density and temperature of the aluminum surface with an applied current of 500 kA.

4. Conclusions

A necessary requirement to deliver sufficient energy to a Pu ICE load on Z to vaporize and disperse material is that a vacuum chamber must exist. The vacuum chamber thus serves as a passive design feature that prevents escape of such material whether or not any other containment feature is functional. If operated in air, circuit simulations show that the Z accelerator could deliver as much as 750 kA into a short-circuit load in the short pulse mode whereas peak current would otherwise be 26 MA with vacuum. For shots with the accelerator operated in a long pulse mode, which is necessary for the ICE shots, we expect a peak current of no greater than 460 kA delivered to a load if operated in air whereas it would be 16 MA with vacuum.

To address the questions about what these low currents could do to an ICE load we used several approaches. These include comparing to a low-current failed shot on Z, estimating the energy loss into a skin-depth of the conductors to determine if there is sufficient to melt or ionize, estimating the peak magnetic pressure and comparing to yield strength, and doing a 2D MHD simulation of this configuration at these low currents.

For an ICE shot on Z when only 450 kA reached the load, but at four times the current density that would be expected with a Pu ICE shot in air at the same current, only minor electrode damage and some melting was seen. But with the Pu ICE configuration even such minor damage is not expected because of its much lower current density. Estimates of energy deposition into the conductors indicate that melting can only occur with peak currents exceeding 1.6 MA. Estimates of the peak pressure on the electrodes show that peak current must be greater than 930 kA for conductor deformation to occur. Finally, these estimates were confirmed with a 2D simulation of the Pu ICE load with a peak current of 500 kA showing that no mechanical deformation occurs, and that electrode temperature only rises 44 K to 337 K, well below melt. Scaling of this temperature rise to melt implies that peak current must be greater than 1.9 MA to start melt.

Thus, if the Pu ICE load were shot with the Z vacuum chamber open, no damage is expected to either the aluminum conductors, or to the plutonium samples. Pressure is not sufficient to plastically deform either the electrodes or the plutonium, but will damage the LiF windows.

5. References

- [1] *J. C. Martin on Pulsed Power*, ed. by T. H. Martin, A. H. Guenther, and M. Kristiansen, Plenum Press, New York (1996), p. 137.
- [2] "Comparison of the Performance of the Upgraded Z with Circuit Predictions", K. W. Struve, L. F. Bennett, J.-P. Davis, M. E. Savage, B. S. Stoltzfus, C. J. Waugh, D. D. Hinshelwood, and T. C. Wagoner, in *Proc. of the 17th IEEE Int. Pulsed Power Conf.*, (2009).
- [3] *Inductance Calculations: Working Formulas and Tables*, F. W. Grover, Dover Publications, Inc., New York (1946), p. 35.
- [4] "Energy Losses in Switches," by T. H. Martin, J. F. Seamen, D. O. Jobe, in the *Proc. of the 9th Int. Pulsed Power Conf.*, 1993, p. 463.
- [5] S. I. Braginskii, "Theory of the Development of a Spark Channel," *JETP*, Vol. 34 (7), No. 6, p. 1068, December 1958.
- [6] *J. C. Martin on Pulsed Power*, op. cit., p. 299.
- [7] S. E. Bronisz, "The Mechanical Properties of Alpha Plutonium in Compression," *J. of Nucl. Materials* **9**, No. 1 (1963) 101-106.
- [8] E. T. Kvamme, D. Trevias, R. Simonson, L. Sokolsky, "A low stress cryogenic mount for space-borne lithium fluoride optics," *Proc. of SPIE Vol. 5877* (SPIE, Bellingham, WA, 2005).
- [9] R. W. Lemke, M. D. Knudson, D. E. Bliss, K. Cochrane, J.-P. Davis, A. A. Giunta, H. C. Harjes, and S. A. Slutz, "Magnetically accelerated, ultrahigh velocity flyer plates for shock wave experiments," *J. of Appl. Physics* **98**, 073530 (2005).

Appendix A. Review of the Peak Current Prediction

Independent review of the peak current prediction by Mark E. Savage, Sandia National Laboratories.

I reviewed your calculations on load current with the Z chamber at atmospheric pressure.

I find your calculations to be conservative if anything. Essentially, you assume that a number of arcs occur around the axis of the machine. Furthermore, you assume that the arcs are far enough apart to have no significant mutual inductance, but are close enough together so that power can flow past. Your first assumption is reasonable; the second assumption is conservative. In fact, I believe that the arcs will be distributed in azimuth because of the inductive voltage drop if they weren't. If the arcs are distributed uniformly, then the magnetic field propagation (current) is evanescent and magnetic field would only extend a distance comparable to the arc separation. The power flow would no longer be TEM, and at distances a few arc spacings away from the arc location, your current estimates are high by one or more e-foldings.

I roughly calculated the temperature rise for 750 kA in a 1 cm width transmission line. The energy density would be 3500 J/cc. Assuming Pu has a heat capacity of 0.4 J/g/K, the temperature rise would be 880 degrees at the surface.

Distribution List

1	MS 1190	Keith Matzen, 1600
1	MS 1191	John Porter, 1670
1	MS 1192	Mike Lopez, 1679
1	MS 1196	Bill Stygar, 1196
1	MS0794	Michael Gruetman, 4126 Steve Coffing Don Steele Robert Matavosian
1	MS0899	Technical Library (electronic copy)